Syntheses and Properties of Nickel(I) and Nickel(II) Complexes of a Series of Macrocyclic N_4 Ligands: Crystal Structures of *C-RSSR*-[Ni^{I}HTIM](ClO_4), *C-RSSR*-[Ni^{II}HTIM](ClO_4)$_2$, *C-RRSS*-[Ni^{II}HTIM](ClO_4)$_2$, and [Ni^{II}TIM](ClO_4)$_2$ (HTIM = 2,3,9,10-Tetramethyl-1,4,8,11-tetraazacyclotetradecane, TIM = 2,3,9,10-Tetramethyl-1,4,8,11-tetraazacyclotetradeca-1,3,8,10-tetraene)

David J. Szalda,[1a,b] Etsuko Fujita,*[,1b] Ralf Sanzenbacher,[1c] Helmut Paulus,[1d] and Horst Elias*[,1c]

Chemistry Department, Brookhaven National Laboratory, Upton, New York 11973-5000, and Eduard-Zintl-Institut für Anorganische Chemie, Technische Hochschule Darmstadt, D-64289 Darmstadt, Federal Republic of Germany

Received March 31, 1994[⊗]

Two isomers of the square-planar nickel(II) complex of 2,3,9,10-tetramethyl-1,4,8,11-tetraazacyclotetradecane (HTIM) were prepared from the nickel(II) complex of 2,3,9,10-tetramethyl-1,4,8,11-tetraazacyclotetradeca-1,3,8,-10-tetraene (TIM) by $NaBH_4$ reduction in aqueous solution. The properties of Ni(II) complexes, Ni(I) complexes, and Ni(I)–CO complexes with a series of 14-membered macrocyclic N_4 ligands were studied by means of UV-vis, NMR, and IR spectroscopy. The CO binding constants range from 1.3×10^2 to 2.8×10^5 M^{-1} at 25 °C in acetonitrile. The crystal structures of *C-RSSR*-[Ni^{I}HTIM]ClO_4 (**1**), *C-RSSR*-[Ni^{II}HTIM](ClO_4)$_2$ (**2**), *C-RRSS*-[Ni^{II}HTIM](ClO_4)$_2$ (**3**) and [Ni^{II}TIM](ClO_4)$_2$ (**4**) have been determined from single-crystal X-ray diffraction data collected by using Mo Kα radiation. Crystallographic data are as follows: (**1**) trigonal space group $R\bar{3}$ with a = 11.971(3) Å, α = 107.46(2)°, V = 1410.3(5) Å^3, Z = 3; (**2**) triclinic space group $P\bar{1}$ with a = 8.503(2) Å, b = 8.438(2) Å, c = 8.028(2) Å, α = 102.63(1)°, β = 104.81(1)°, γ = 101.76(1)°, V = 522.4(4) Å^3, Z = 1; (**3**) monoclinic space group $P2_1/c$ with a = 8.307(4) Å, b = 12.521(6) Å, c = 10.587(6) Å, β = 103.66(2)°, V = 1070(2) Å^3, Z = 2; (**4**) orthorhombic space group *Pnma* with a = 13.189(2) Å, b = 11.672(2) Å, c = 13.757(3) Å, V = 2118(1) Å^3, Z = 4. All complexes have square-planar geometry and the stereochemistry of the four coordinating N atoms in complexes (**1**), (**2**), and (**3**) is *Trans III*. Although the two sets of Ni–N distances of 2.083(3) and 2.053(3) Å for the Ni(I) complex, (**1**), are much longer than those of 1.969(1) and 1.948(2) Å for the corresponding Ni(II) complex, (**2**), distortion of the macrocycle core was not observed upon the reduction of the metal center. The structural changes associated with the reduction of Ni(II) to Ni(I) in square-planar complexes can be classified in three ways: (1) expansion of Ni–N distances; (2) distortion of nickel core; (3) both expansion and distortion.

Introduction

Because of great interest[2] in carbon dioxide fixation and utilization, the reduction chemistry of nickel porphyrins, hydroporphyrins, and 14-membered tetraazamacrocyclic complexes as models for F430 and as catalysts for CO_2 reduction has recently received a lot of attention.[2-10] F430 is a nickel(II) hydrocorphin and the prosthetic group of methyl coenzyme M reductase, which catalyzes the reductive cleavage of S-methyl coenzyme M to coenzyme M and methane in the final step of the reduction of carbon dioxide to methane in methanogenic bacteria.[3] Involvement of nickel(I) has been proposed for methane production by F430 and the CO_2 reduction by nickel tetraazamacrocyclic complexes.

Nickel tetraazamacrocyclic complexes catalyze the electrochemical[4-6] and photochemical[6-8] reduction of CO_2 to produce CO. Beley et al. reported that [Nicyclam]$^{2+}$ is remarkably efficient and selective for electrochemical reduction of CO_2 to CO, even in H_2O. The importance of the adsorbed [Ni^{I}cyclam]$^+$ proposed by the authors was further studied by two groups.[9,10] Although the [Nicyclam-CO_2]$^+$ and [Nicyclam-COOH]$^{2+}$ complexes received extensive attention as intermediates of the electrochemical CO_2 reduction,[5,7,11] these species have not yet been characterized.

On the other hand, Ni(I) macrocyclic complexes and their CO adducts have been prepared, *in situ*, and their electronic absorption, ESR, and IR spectra have been measured.[5,12-21] However, there have been only few reports on the crystal structures of Ni(I) complexes.[20-22]

The structural consequences associated with the reduction of Ni(II) in porphyrins, hydroporphyrins,[23] F430[24] and F430M[25] (the pentamethyl ester of F430) have been recently studied by EXAFS. The larger core size of the Ni^{I} complex compared to that of the Ni^{II} square-planar complex can be explained by an additional electron in the $d_{x^2-y^2}$ orbital and a decrease of the ligand-field strength. However, an EXAFS study of Ni(I) isobacteriochlorin, F430 and F430M indicated a distortion of the nitrogens around the metal together with an expansion of the coordination core. For example, low spin Ni(II) F430M has a Ni–N bond length of 1.90(2) Å and the reduced species, Ni(I) F430M, has two distinct sets of Ni(I)–N distances of 1.88 (3) and 2.03(3) Å with an average expansion of 0.06 Å. The

[⊗] Abstract published in *Advance ACS Abstracts,* November 1, 1994.

(1) (a) Permanent address: Department of Natural Sciences, Baruch College, Manhattan, NY10010. (b) Brookhaven National Laboratory. (c) Darmstadt. (d) Darmstadt, Fachbereich Materialwissenschaft.

(2) (a) *Catalytic Activation of Carbon Dioxide*; Ayers, W. M., Ed.; ACS Symposium Series 363; American Chemical Society: Washington, DC, 1988; Vol. 363. (b) *Electrochemical and Electrocatalytic Reduction of Carbon Dioxide*; Sullivan, B. P., Ed; Elsevier: Amsterdam, 1993. (c) Proceedings of the International Symposium on Chemical Fixation of Carbon Dioxide, Nagoya, Japan, 1991. (d) Proceedings of the International Conference on Carbon Dioxide Utilisation, Bari, Italy, 1993.

0020-1669/94/1333-5855$04.50/0

Chart 1

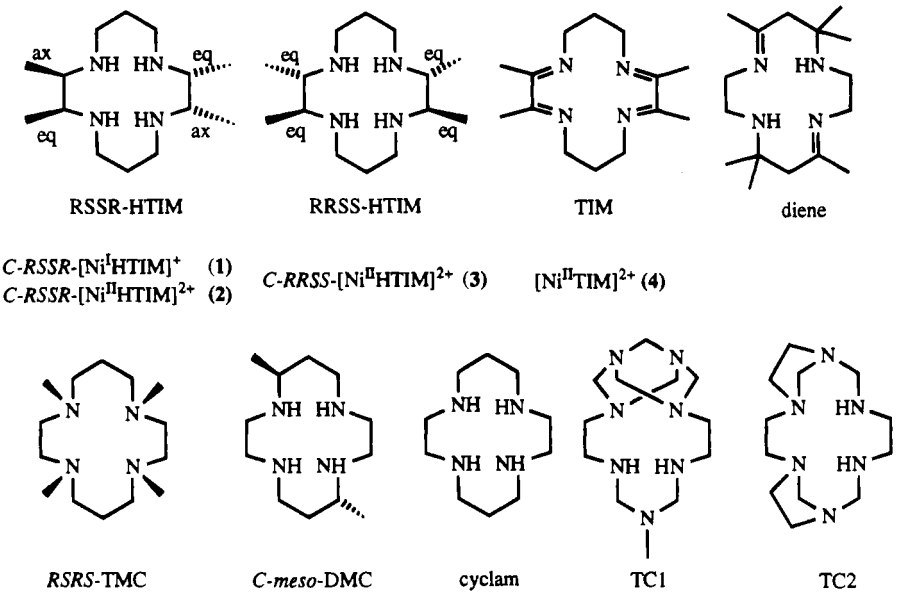

validity of the EXAFS analyses was supported by our single crystal structure studies of Ni(II) and Ni(I) complexes of diene (diene = 5,7,7,12,14,14-hexamethyl-1,4,8,11-tetraazacyclotetradeca-4,11-diene).[20,26] The Ni(II)−N_{imine} and Ni(II)−N_{amine} distances of 1.907(2) and 1.938(2) Å, respectively, in the square-planar [Ni^{II}diene]$(ClO_4)_2$ complex are in good agreement with the EXAFS data of 1.93 Å in CH_3CN. The Ni(I)−N_{imine} distances are 1.988(7) and 1.979(7) Å and the Ni(I)−N_{amine} distances are 2.063(6) and 2.068(6) Å, which are also in good agreement with the EXAFS data (two sets of the bond lengths of 1.97 and 2.06 Å) and are longer than those for the corresponding Ni(II) complex. The average expansion is 0.10 Å and the difference between the two sets of bonds increases by 0.05 Å.

Chart 2

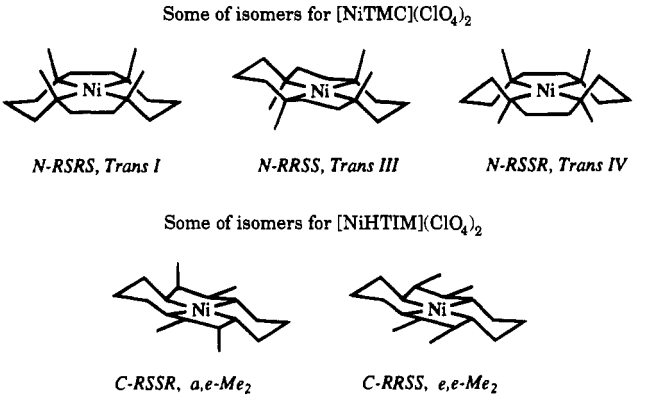

Recently Suh and her co-workers have reported the X-ray crystal structures of the nickel (I) complexes of TC1 (8-methyl-

(3) (a) Gulsalus, R. P.; Wolfe, R. S. *J. Bacteriol.* **1978**, *135*, 851. (b) Ellefson, W. L.; Whitman, W. B.; Wolfe, R. S. *Proc. Natl. Acad. Sci. U.S.A.* **1982**, *79*, 3707. (c) Livingston, D. A.; Pfaltz, A.;Schreiber, J.; Eschenmoser, A.; Ankel-Fuchs, D.; Moll, J.; Jaenchen, R.; Thauer, R. K. *Helv. Chim. Acta* **1984**, *67*, 334. (d) Fässler, A.; Kobelt, A.; Pfaltz, A.; Eschenmoser, A.; Bladon, C.; Battersby, A. R.; Thauer, R. K. *Helv. Chim. Acta* **1985**, *68*, 2287. (e) Daniels, L.; Sparling, R.; Sprott, G. D. *Biochem. Biophys.* **1984**, *768*, 113. (f) Pfaltz, A.; Jaun, B.; Fässler, A.; Eschenmoser, A.; Jaenchen, R.; Gilles, H.; Diekert, G.; Thauer, R. K. *Helv. Chim. Acta* **1982**, *65*, 828. (g) Won, H.; Olson, K. D.; Wolfe, R. S.; Summers, M. F. *J. Am. Chem. Soc.* **1990**, *112*, 2178. (h) Albracht, S. P. J.; Ankel-Fuchs, D.; Van der Zwaan, J. W.; Fontijn, R. D.; Thauer, R. K. *Biochim. Biophys. Acta* **1986**,*870*, 57. (i) Jaun, B.; Pfaltz, A. *J. Chem. Soc., Chem. Commun.* **1986**, 1327. (j) Jaun, B.; Pfaltz, A. *J. Chem. Soc., Chem. Commun.* **1988**, 293. (k) Pfaltz, A.; Livingston, D. A.; Jaun, B.; Diekert, G.; Thauer, R. K.; Eschenmoser, A. *Helv. Chim. Acta* **1985**, *68*, 1338. (l) Shiemke, A. K.; Hamilton, C. L.; Scott, R. A. *J. Biol. Chem.* **1988**, *263*, 5611. (m) Rouvière, P. E.; Wolfe, R. S. *J. Biol. Chem.* **1988**, *263*, 7913. (n) Won, H.; Olson, K. D.; Summers, M. F.; Wolfe, R. S. *Comments Inorg. Chem.* **1993**, *15*, 1−26. (o) Färber, G.; Keller, W.; Kratky, C.; Juan, B.; Pfaltz, A.; Spinner, C.; Kobelt, A.; Eschenmoser, A. *Helv. Chim. Acta* **1991**, *74*, 697. (p) Holliger, C.; Pierik, A. J.; Reijerse, E. J.; Hagen, W. R. *J. Am. Chem. Soc.* **1993**, *115*, 5651. (q) Hamilton, C. L.; Ma, L.; Renner, M. W.; Scott, R. A. *Biochim, Biophys. Acta* **1991**, *1074*, 312.

(4) Fisher, B.; Eisenberg, R. *J. Am. Chem. Soc.* **1980**, *102*, 7361.

(5) Beley, M.; Collin, J. P.; Ruppert, R.; Sauvage, J. P. *J. Am. Chem. Soc.* **1986**, *108*, 7461.

(6) Tinnermans, A. T. A.; Koster, T. P. M.; Thewissen, D. H. M. W.; Mackor, A. *Recl. Trav. Chim. Pays. -Bas* **1984**, *103*, 288−295.

(7) Grant, J. L.; Goswami, K.; Spreer, L. O.; Otvos, J. W.; Calvin, M. *J. Chem. Soc., Dalton Trans* **1987**, 2105.

(8) Craig, C. A.; Speer, L. O.; Otvos, J. W.; Calvin, M. *J. Phys. Chem.* **1990**, *94*, 7957.

(9) (a) Fujihira, M.; Hirata, Y.; Suga, K. *J. Electroanal. Chem.* **1990**, *292*, 199−215. (b) Fujihira, M.; Nakamura, Y.; Hirata, Y.; Akiba, U.; Suga, K. *Denki Kagaku* **1991**, *59*, 532.

(10) (a) Balazs, G. B.; Anson, F. C. *J. Electroanal. Chem.* **1992**, *322*, 325−345. (b) Balazs, C. B.; Anson, F. C. *J. Electroanal. Chem.* **1993**, *361*, 149−157.

(11) Sakaki, S. *J. Am. Chem. Soc.* **1992**, *114*, 2055−62.

(12) Olson, D. C.; Vasilevskis, J. *Inorg. Chem.* **1969**, *8*, 1611.

(13) Lovecchio, F. V.; Gore, E. S.; Busch, D. H. *J. Am. Chem. Soc.* **1974**, *96*, 3109.

(14) Jubran, N.; Ginzburg, G.; Cohen, H.; Koresh, Y.; Meyerstein, D. *Inorg. Chem.* **1985**, *24*, 251−258.

(15) Jubran, N.; Meyerstein, D.; Cohen, H. *J. Chem. Soc., Dalton Trans.* **1986**, 2509.

(16) (a) Jubran, N.; Meyerstein, D.; Cohen, H. *Inorg. Chim. Acta* **1986**, *117*, 129−132. (b) Jubran, N.; Ginzburg, G.; Cohen, H.; Meyerstein, D. *J. Chem. Soc., Chem. Commun.* **1982**, 517.

(17) Gagné, R. R.; Ingle, D. M. *Inorg. Chem.* **1981**, *20*, 420.

(18) Bakac, A.; Espenson, J. H. *J. Am. Chem. Soc.* **1986**, *108*, 713.

(19) Ram, M. S.; Bakac, A.; Espenson, H. *Inorg. Chem.* **1986**, *25*, 3267.

(20) Furenlid, L. R.; Renner, M. W.; Szalda, D. J.; Fujita, E. *J. Am. Chem. Soc.* **1991**, *113*, 883.

(21) Suh, M. P.; Kim, H. K.; Kim, M. J.; Oh, K. Y. *Inorg. Chem.* **1992**, *31*, 3620−3625.

(22) Latos-Grazynski, L.; Olmstead, M. M.; Balch, A. L. *Inorg. Chem.* **1989**, *28*, 4066.

(23) Furenlid, L. R.; Renner, M. W.; Smith, K. M.; Fajer, J. *J. Am. Chem. Soc.* **1990**, *112*, 1634.

(24) Shiemke, A. K.; Kaplan, W. A.; Hamilton, C. L.; Shelnutt, J. A.; Scott, R. A. *J. Biol. Chem.* **1989**, *264*, 7276−7284.

(25) Furenlid, L. R.; Renner, M. W.; Fajer, J. *J. Am. Chem. Soc.* **1990**, *112*, 8987−8989.

(26) Szalda, D. J.; Fujita, E. *Acta Cryst.* **1992**, *C48*, 1767−1771.

1,3,6,8,10,13,15-heptaazatricyclo[13.1.1.1^{13,15}]octadecane) and TC2 (1,3,6,9,11,14-hexaazamacrotricyclo[12.2.1.1.^{6,9}]octadecane)[21,27,28] (see Chart 1). The two structures show two sets of Ni−N distances, each set consisting of two cis Ni−N bonds involving a six-membered chelate ring, rather than a simple expansion of the macrocycle core. In fact, the expansions of the cores in the two structures are almost negligible compared to that of [Nidiene]$^{+/2+}$ (the difference of the averaged Ni(I)−N and Ni(II)−N: −0.003 Å for [NiTC1]$^{+/2+}$; 0.012 Å for [NiTC2]$^{+/2+}$; 0.103 Å for [Nidiene]$^{+/2+}$).

In order to determine the origin of the occurrence of the two sets of Ni−N distances and the core size change upon the reduction, we extended our work to the complexes with more symmetric ligands. In this paper, we describe the preparation and properties of square-planar Ni(II) complexes, square-planar Ni(I) complexes, and square pyramidal Ni(I)−CO complexes with a series of 14-membered macrocyclic N_4 ligands as well as the X-ray crystal structures of *C-RSSR*-[Ni^{I}HTIM](ClO$_4$) (**1**), *C-RSSR*-[Ni^{II}HTIM](ClO$_4$)$_2$ (**2**), *C-RRSS*-[Ni^{II}HTIM](ClO$_4$)$_2$ (**3**), and [Ni^{II}TIM](ClO$_4$)$_2$ (**4**). The configuration isomers[29] for [NiTMC](ClO$_4$)$_2$, (TMC = 1,4,8,11-tetramethyl-1,4,8,11-tetraazacyclotetradecane) and [NiHTIM](ClO$_4$)$_2$ are shown in Chart 2 for clarity.

Experimental Section

Materials. All solvents and reagents were used without further purification unless mentioned. Acetonitrile was purified by published methods and stored under vacuum over activated molecular sieves (3A) or CaH_2.[32] Research grade CO (>99.997% pure) and CO_2 (>99.998% pure) were used without further purification. *RSRS*-[NiTMC](ClO$_4$)$_2$,[33,34] (*Trans I* form), [NiTIM](ClO$_4$)$_2$,[35] and [Nicyclam](ClO$_4$)$_2$ (cyclam = 1,4,8,11-tetraazacyclotetradecane)[36] were prepared as previously described and characterized by UV-vis, IR and NMR spectroscopy. Nickel and anion analyses were satisfactory. (***Warning**: The perchlorate salts used in this study may be explosive and potentially hazardous.*)

Preparation of *C-RSSR*-[Ni^{II}HTIM](ClO$_4$)$_2$ (2) and *C-RRSS*-[Ni^{II}HTIM](ClO$_4$)$_2$ (3). 15.2 g (30 mmol) of [Ni^{II}TIM](ClO$_4$)$_2$ (**4**) are suspended in 400 mL water with stirring and cooling to 5 °C. Within 2 h, 6.8 g (180 mmol) $NaBH_4$ are added in small portions, whereupon complex (**4**) dissolves and the color of the solution changes from orange to green-brown and finally to yellow. After heating to 90 °C for 15 min the hot solution is filtered (separation of small amounts of a black solid, most probably Ni) and set to pH 3 by addition of $HClO_4$ (70%). The raw product crystallizes upon cooling in a refrigerator. The orange crystals are separated by filtration, washed with a little ethanol and ether and dried (yield, 40−70%). The raw product, a mixture of various stereoisomers of [Ni^{II}HTIM](ClO$_4$)$_2$, is recrystallized from nitromethane. The solid fraction thus obtained is subjected to two more recrystallization steps in nitromethane, which leads to orange-red crystals of (**3**)·nitromethane. The crystals are dried in vacuo to remove the nitromethane and recrystallized from MeOH/H_2O (v/v = 4) to give the orange-red isomer (**3**) (yield 30%, referring to the raw product). The filtrate of the first recrystallization of the raw product from nitromethane is taken to dryness and the solid residue is recrystallized three times from MeOH/H_2O (v/v = 4) to obtain orange-red crystals of isomer (**2**) (yield 10%, referring to the raw product). The X-ray powder diffraction spectra of (**2**) and (**3**) agreed with those calculated from the single crystal X-ray diffraction data. It was thus confirmed that (**2**) is the RSSR isomer and (**3**) the RRSS isomer. One can estimate from the yields that (**3**) and (**2**) are present in the raw product at a ratio of 2:1.[37] Anal. Calcd for $C_{14}H_{32}Cl_2N_4NiO_8$: C, 32.71; H, 6.27; N, 10.90. Found: C, 32.55; H, 6.48; N, 10.87. ^{13}NMR of (**2**) in CD_3NO_2: δ 9.93 (2C, CH_3), 12.89 (2C, CH_3), 26.86 (2C, $NCH_2CH_2CH_2N$), 46.65 (2C, NCH_2CH_2), 47.15 (2C, NCH_2CH_2), 60.87 (2C, CHN), 61.84(CHN) ppm (standard: TMS at 0 ppm). ^{13}NMR of (**3**) in CD_3NO_2: δ 16.19 (4C, CH_3), 27.38 (2C, $NCH_2CH_2CH_2N$), 47.91 (4C, NCH_2CH_2), 64.36 (4C, CHN) ppm (standard: TMS at 0 ppm).

Preparation of *C-meso*-[Ni^{II}DMC](ClO$_4$)$_2$. The unsaturated precursor of the ligand, 5,12-dimethyl-1,4,8,11-tetraazacyclotetradeca-4,11-diene, was prepared as reported[38a] by using "method B". The preparation of DMC by hydrogenation of this precursor and the separation of the C-meso-isomer of DMC from the C-rac-isomer was carried out according to the literature[38b] with the melting point being used for purity control. As long as the melting point is lower than reported[38b] (144 °C) further recrystallization from xylene is necessary to obtain pure *C-meso*-DMC. The thermodynamically most stable isomer of *C-meso*-[Ni^{II}DMC](ClO$_4$)$_2$ was prepared in a slightly basic medium according to the following procedure: A solution of Ni(ClO$_4$)$_2$·6H_2O (1 mmol) in 20 mL dried methanol is added dropwise to a hot solution of 1.05 mmol of *C-meso*-DMC in 20 mL of dried methanol while stirring. After refluxing for 30 min and the addition of a few drops of concentrated $HClO_4$ (in order to dissolve small amounts of a green precipitate, most probably Ni(OH)$_2$) the solution is cooled, whereupon the orange-red complex begins to crystallize (yield, 70%). It is recrystallized from methanol containing 4% water.

Spectroscopic Measurements. The Ni^{I} complex was prepared by sodium amalgam (Na−Hg) reduction from the Ni^{II} complex in CH_3CN or CD_3CN and the Ni^{I}−CO complex by the introduction of CO (room temperature, atmospheric pressure) into solutions of the Ni^{I} complexes. Infrared samples of nickel complexes (0.01−0.05 M Ni) were prepared by syringe transfer of the solution to an Ar- or CO-flushed, vacuum-tight IR cell (0.5 mm path length, CaF_2 windows). Spectra were immediately determined on a Mattson Polaris FT-IR spectrometer. UV-vis spectra were measured in sealed cells under vacuum or a CO atmosphere on a Hewlett Packard 8452 A spectrophotometer and a Cary 210 spectrophotometer. NMR spectra were obtained on a Bruker AM-300 300 MHz spectrometer. The powder diffraction spectra were measured on a Stoe-Powder Diffraction System (type 6.11.1).

For the Ni^{II} complexes, low-spin square-planar and high-spin distorted octahedral species coexist in the solution according to reactions 1 and 2. The equilibrium was studied by spectrophotometric titration

$$\underset{\text{low spin}}{\text{NiL}} + CH_3CN \rightleftharpoons \underset{\text{high spin}}{\text{NiL}(CH_3CN)} \qquad K_1 \quad (1)$$

$$\text{NiL}(CH_3CN) + CH_3CN \rightleftharpoons \underset{\text{high spin}}{\text{NiL}(CH_3CN)_2} \qquad K_2 \quad (2)$$

$$\beta = K_1K_2 \quad (3)$$

of solutions of the Ni^{II} complex (NiL) in CH_3NO_2 with CH_3CN at 380−

(27) Suh, M. P.; Shin, W.; Kim, H.; Koo, C. H. *Inorg. Chem.* **1987**, *26*, 1846−1852.
(28) Suh, M. P.; Kang, S.; Goedken, V. L.; Park, S. *Inorg. Chem.* **1991**, *30*, 365−370.
(29) The original synthesis and the names (*Trans I-V*) of five possible diastereomers of Nicyclam complexes were given by Bosnich et al.[30] The Cahn-Prelog-Ingold designation of the nitrogen configurations or the carbon configurations as *C-RRSS* indicates their chirality.[31] It should be noted that the ligand HTIM possesses four chiral C atoms and, upon coordination, four chiral N atoms. In the present paper the stereochemistry resulting from C-chirality and N-chirality is characterized by the use of the prefix "C" (e.g., *C-RRSS*-HTIM) and "N" (e.g., N-*RSRS*-TMC), respectively.
(30) Bosnich, B.; Poon, C. K.; Tobe, M. I. *Inorg. Chem.* **1965**, *4*, 1102.
(31) Barefield, E. K.; Bianchi, A.; Billo, E. J.; Connolly, P. J.; Paoletti, P.; Summers, J. S.; Van Derveer, D. G. *Inorg. Chem.* **1986**, *25*, 4197.
(32) Riddick, J. A.; Bunger, W. B.; Sakano, T. K. *Organic Solvents, Physical Properties and Methods of Purification;* 4th ed.; Wiley: New York, 1986.
(33) Barefield, E. K.; Wagner, F. *Inorg. Chem.* **1973**, *12*, 2435−2439.
(34) Wagner, F.; Mocella, M. T.; D'Aniello, M. J., Jr.; Wang, A. H.-J.; Barefield, E. K. *J. Am. Chem. Soc.* **1974**, *96*, 2625.
(35) *Inorganic Synthesis*; Douglas, B. E., Ed.; Wiley: New York; Vol. XVIII.
(36) Bosnich, B.; Tobe, M. I.; Webb, G. A. *Inorg. Chem.* **1965**, *4*, 1109.
(37) Note added in proof: After submission of the manuscript HPLC techniques were applied to separate the isomers from the raw product. The results so far obtained confirm that (**3**) is the main isomer. It is found however that, in addition to (**3**) and (**2**), three more isomers can be separated, albeit in low yields.

Table 1. Crystallographic Data for *C-RSSR*-[NiHTIM](ClO$_4$) (**1**), *C-RSSR*-[NiHTIM](ClO$_4$)$_2$ (**2**), *C-RRSS*-[NiHTIM](ClO$_4$)$_2$ (**3**), and [NiTIM](ClO$_4$)$_2$ (**4**)

	(1)	(2)	(3)	(4)
formula	[Ni($N_4C_{14}H_{32}$)]ClO$_4$	[Ni($N_4C_{14}H_{32}$)](ClO$_4$)$_2$	[Ni($N_4C_{14}H_{32}$)](ClO$_4$)$_2$	[Ni($N_4C_{14}H_{24}$)](ClO$_4$)$_2$·H_2O
a, Å	11.971(3)	8.503(2)	8.307(4)	13.189(2)
b, Å	11.971(3)	8.438(2)	12.521(6)	11.672(2)
c, Å	11.971(3)	8.028(2)	10.587(6)	13.757(3)
α, deg	107.46(2)	102.63(1)		
β, deg	107.46(2)	104.81(1)	103.66(2)	
γ, deg	107.46(2)	101.76(1)		
V, Å^3	1410.3(5)	522.4(4)	1070(2)	2118(1)
Z	3	1	2	4
fw	414.58	514.05	514.05	523.99
space group	$R\bar{3}$	$P\bar{1}$	$P2_1/c$	*Pnma*
ϱ(calcd), g cm^{-3}	1.464	1.634	1.595	1.643
λ, Å (graphite monochromatized)	0.710 69 (Mo Kα)	0.710 69 (Mo Kα)	0.710 69 (Mo Kα)	0.710 69 (Mo Kα)
μ, cm^{-1}	12.0	12.3	12.0	12.2
transm coeff	0.565−0.656	0.673−0.782	0.615−0.921	0.878−0.929
R^a	0.048	0.033	0.035	0.069
$R_w{}^a$	0.069	0.032	0.030	0.084
max shift/error final cycle	≤0.01	≤0.15	≤0.015	≤0.1
T, K	295	303	291	295

^{a} $R = \sum||F_o| - |F_c||/\sum|F_o|$; $R_w = \{\sum[w(|F_o| - |F_c|)^2]/\sum[w|F_o|^2]\}^{1/2}$.

800 nm at 25 °C. The data obtained for the absorbance A at 454 nm for [Nicyclam]$^{2+}$, 460 nm for [NiHTIM]$^{2+}$ and 466 nm for [NiDMC]$^{2+}$, were fitted to eq 4, where A_o, A_i, and A_f are the absorbance of the species

$$A = (A_o + A_iK_1[CH_3CN] + A_f\beta[CH_3CN]^2)/(1 + K_1[CH_3CN] + \beta[CH_3CN]^2) \quad (4)$$

NiL^{2+}, NiL(CH$_3$CN)$^{2+}$, and NiL(CH$_3$CN)$_2{}^{2+}$, respectively. The number of data points was at least 10 in each titration.

Electrochemistry and Binding Constant Measurements. CO binding constants were determined by previously described cyclic voltammetry techniques.[20,39,40] Cyclic voltammograms in CH$_3$CN were obtained on a BAS100 electrochemical analyzer with scan rates ranging from 2 to 100 mV s^{-1} using a conventional H-type cell. Solutions contained 1 mM nickel complex and 0.1 M tetrapropylammonium perchlorate in dry CH$_3$CN and gas compositions of 0, 20, 50, 100% CO in Ar. Graphite, Pt and SCE were used as working, counter and reference electrodes, respectively. Ferrocene was used as an internal standard. The solubility of CO in CH$_3$CN at 25 °C was previously determined to be 0.0083 M.[41]

Collection and Reduction of X-ray Data. Crystals of *C-RSSR*-[NiHTIM](ClO$_4$) (**1**), prepared by very slow removal of CH$_3$CN under vacuum, were very deep purple blocks. A crystal 0.45 × 0.45 × 0.50 mm was coated with petroleum jelly and placed in a capillary tube. The diffraction data indicated trigonal symmetry with no systematic absences. Space group $R\bar{3}$ (No. 148) was assumed for the solution and refinement of the crystal structure.[42,43]

Crystals of *C-RSSR*-[NiHTIM](ClO$_4$)$_2$ (**2**), obtained by slow evaporation of an aqueous solution of (**2**) in a desiccator, were orange rhombic plates. A crystal 0.27 × 0.35 × 0.40 mm was mounted on a glass fiber. The diffraction data indicated triclinic symmetry and space group $P\bar{1}$ (No. 2) was assumed for the solution and refinement of the crystal structure.[42,43]

Table 2. Positional Parameters^a and U_{eq} Values (Å^2) for the Non-Hydrogen Atoms in *C-RSSR*-[NiHTIM](ClO$_4$) (**1**)

atom	x	y	z	U_{eq}
Ni	0.0000	0.5000	0.0000	0.024
N1	0.2000(3)	0.5666(3)	0.0939(3)	0.032
C2	0.2244(4)	0.5517(4)	0.2164(3)	0.040
C22	0.3629(5)	0.5722(6)	0.2907(4)	0.065
C3	0.1244(4)	0.4175(4)	0.1831(3)	0.038
C33	0.1381(5)	0.3082(4)	0.0916(4)	0.047
N4	−0.0052(3)	0.4141(3)	0.1244(3)	0.031
C5	−0.1151(4)	0.2884(4)	0.0742(5)	0.047
C6	−0.2437(4)	0.2920(4)	0.0160(5)	0.048
C7	−0.2751(4)	0.3015(4)	−0.1115(4)	0.046
Cl1	0.0000	0.5000	0.5000	0.059
O11	0.1024(10)	0.5341(13)	0.4599(11)	0.095
O12	−0.1171(8)	0.4518(9)	0.3610(8)	0.081
O13	−0.0035(11)	0.6205(10)	0.5649(10)	0.082
O14	−0.0267(17)	0.4130(16)	0.534(2)	0.152

^{a} Numbers in parentheses are errors in the last significant digit(s). $U_{eq} = {}^1/_3\sum_i\sum_j U_{ij}a^*_i a^*_j \mathbf{a}_i\cdot\mathbf{a}_j$.

Crystals of *C-RRSS*-[NiHTIM](ClO$_4$)$_2$ (**3**), obtained by slow crystallization from methanol, were orange plates. A crystal 0.075 × 0.55 × 0.60 mm was mounted on a glass fiber. The diffraction data indicated the crystal to be monoclinic with systematic absences $0k0$, $k = 2n + 1$ and $h0l$, $l = 2n + 1$ consistent with space group $P2_1/c$ (No. 14).[42,43]

Crystals of [NiTIM](ClO$_4$)$_2$ (**4**), prepared by slow evaporation of the solvent from the CH$_3$NO$_2$ solution, were golden brown prisms. A crystal 0.06 × 0.30 × 0.50 mm was mounted on a glass fiber. The diffraction data indicated orthorhombic symmetry with systematic absences $h0l$, $h + l = 2n + 1$ and $hk0$, $k = 2n + 1$ consistent with the space groups $P2_1nb$ and $Pmnb$ non standard settings of space groups $Pna2_1$ (No. 33) and *Pnma* (No. 62).[42] Solution and refinement of the structure indicated the centrosymmetric space group so the crystal parameters and intensity data were converted to the space group *Pnma*. All the parameters in this paper for this structure refer to this space group.

Crystal data and information on data collection for all four structures are given in Table 1 and, in detail, in Table S1.

Determination and Refinement of Structure. The structures of (**1**) and (**4**) were solved by standard Patterson heavy-atom methods.[43a] The structure of (**2**) and (**3**) were solved using SHELXS86 (TREF).[43b] In the full-matrix least-squares refinement, neutral-atom scattering factors[44] and corrections for anomalous dispersion were used and the

(38) (a) Kolinski, R. A.; Korybut-Daszkiewicz, B. *Bull. Acad. Pol. Sci. Ser. Sci. Chim.* **1969**, *17*, 13. (b) Hay, R. W.; Piplani, D. P. *J. Chem. Soc., Dalton Trans.* **1977**, 1956.
(39) Bard, A. J.; Faulkner, L. R. *Electrochemical Methods, Fundamentals and Application*; John Wiley & Sons, Inc.: New York, 1980, p 34.
(40) Gagné, R. R.; Allison, J. L.; Inble, D. M. *Inorg. Chem.* **1979**, *18*, 2767.
(41) Fujita, E.; Creutz, C.; Sutin, N.; Szalda, D. J. *J. Am. Chem. Soc.* **1991**, *113*, 343−353.
(42) (a) *International Tables for X-ray Crystallography;* 3rd ed.; Kynoch Press: Birmingham, England, 1969; Vol. I. p 253. (b) *Ibid.* Vol. I, p 75. (c) *Ibid.* Vol. I, p 99. (d) *Ibid.* Vol. I, p 119. (e) *Ibid.* Vol. I, p 151.
(43) (a) Sheldrick, G. M., 1976, SHELX 76, Crystal Structure refinement program, Cambridge University, England. (b) Sheldrick, G. M. *Acta Crystallogr.* **1990**, *A46*, 467−473.
(44) Neutral atom scattering factors were taken from International Tables for X-ray Crystallography, Kynoch Press, Birmingham, England, 1974, Vol. IV, pp 99−100. Anomalous dispersion effects were taken from: Cromer, D. T., Weiman, D. *J. Chem. Phys.* **1970**, *53*, 1891−1898.

Table 3. Positional Parameters[a] and U_{eq} Values (Å^2) for the Non-Hydrogen Atoms[b] in *C-RSSR*-[NiHTIM](ClO$_4$)$_2$ (**2**)

atom	*x*	*y*	*z*	U_{eq}
Ni	0.5000	0.5000	0.5000	0.023
N1	0.3010(2)	0.3277(2)	0.3214(2)	0.024
C2	0.3179(2)	0.1587(2)	0.3398(2)	0.026
C22	0.1608(3)	0.0118(3)	0.2326(3)	0.037
C3	0.3725(2)	0.1783(2)	0.5405(2)	0.026
C33	0.2361(2)	0.2043(3)	0.6266(6)	0.034
N4	0.5279(2)	0.3243(2)	0.6180(2)	0.024
C5	0.5952(2)	0.3661(3)	0.8169(2)	0.033
C6	0.7616(2)	0.5015(3)	0.8913(3)	0.035
C7	0.7430(3)	0.6708(3)	0.8702(2)	0.033
Cl1	0.77980(10)	0.25890(10)	0.28570(10)	0.038
O1	0.6741(2)	0.3672(2)	0.2579(3)	0.054
O2	0.7957(3)	0.2277(3)	0.4559(3)	0.059
O3	0.9331(3)	0.3158(4)	0.2560(4)	0.065
O4	0.6947(4)	0.0975(3)	0.1540(4)	0.088
O5A	0.9540(15)	0.3846(14)	0.3332(14)	0.053
O5B	0.834(4)	0.327(4)	0.483(4)	0.052
O5C	0.788(3)	0.151(3)	0.160(3)	0.056

[a] Numbers in parentheses are errors in the last significant digit(s). [b] Site occupancy factors for O3, O4, O5A, O5B, and O5C are 0.77, 0.87, 0.20, 0.06, and 0.10, respectively. $U_{eq} = {}^1/_3\sum_i\sum_j U_{ij}a^*_i a^*_j \mathbf{a}_i\cdot\mathbf{a}_j$.

Table 4. Positional Parameters[a] and U_{eq} Values (Å^2) for the Non-Hydrogen Atoms in *C-RRSS*-[NiHTIM](ClO$_4$)$_2$ (**3**)

atom	*x*	*y*	*z*	U_{eq}
Ni	0.0000	0.0000	0.0000	0.030
N1	0.1937(3)	−0.0854(2)	−0.0021(3)	0.035
C2	0.3105(4)	−0.0890(3)	0.1280(3)	0.040
C22	0.4236(4)	−0.1876(3)	0.1444(4)	0.055
C3	0.2107(4)	−0.0841(3)	0.2288(3)	0.043
C33	0.3162(5)	−0.0659(4)	0.3648(4)	0.079
N4	0.0797(3)	−0.0009(2)	0.1880(3)	0.036
C5	−0.0424(4)	−0.0097(3)	0.2698(3)	0.046
C6	−0.1761(4)	0.0733(3)	0.2385(3)	0.047
C7	−0.2848(4)	0.0614(3)	0.1041(3)	0.046
Cl1	0.17800(10)	0.27330(10)	0.00720(10)	0.047
O1	0.2691(3)	0.3622(2)	0.0665(3)	0.071
O2	0.0136(3)	0.2789(2)	0.0287(3)	0.079
O3	0.2575(4)	0.1781(2)	0.0619(3)	0.090
O4	0.1685(4)	0.2750(3)	−0.1291(3)	0.090

[a] Numbers in parentheses are errors in the last significant digit(s). $U_{eq} = {}^1/_3\sum_i\sum_j U_{ij}a^*_i a^*_j \mathbf{a}_i\cdot\mathbf{a}_j$.

quantity $\sum w(|F_o| - |F_c|)^2$ was minimized. Anisotropic temperature parameters were used for all the non-hydrogen atoms (except for the disordered oxygen atoms of the perchlorate ion in (**2**)). For (**1**) hydrogen atoms were found on a difference Fourier map and included in the refinement in fixed positions. For (**2**), (**3**) and (**4**) during the final cycles of refinement, hydrogen atoms were introduced in their calculated positions and allowed to "ride"[43] on the C or N atom to which they were bound (except for the hydrogen atoms attached to the nitrogen of the macrocycle in (**2**) and (**3**) which were refined and the hydrogen atoms on the water in (**4**) which were not included). A common isotropic thermal parameter was refined for all of the hydrogens in (**1**) and (**4**). For (**3**) the isotropic thermal parameter for the calculated hydrogen atoms was fixed at 1.1 times the equivalent isotropic parameter of the connecting C or N atom. In (**2**) the isotropic thermal parameters of the hydrogen atoms calculated for each C or N atom were treated as in (**3**) except the multiplicative factor was refined by least squares to a value of 1.18. The atomic coordinates for the non-hydrogen atoms are listed in Tables 2−5. Bond lengths and angles are summarized in Table 6.

Results

Structures. A view of the cations of *C-RSSR*-[NiHTIM]-(ClO$_4$) (**1**) and *C-RSSR*-[NiHTIM](ClO$_4$)$_2$ (**2**) can be seen in Figures 1 and 2, respectively. The atom labeling scheme used is presented in the figures with the unlabeled atoms being related

Table 5. Positional Parameters[a] and U_{eq} Values (Å^2) for the Non-Hydrogen Atoms in [NiTIM](ClO$_4$)$_2$ (**4**)

atom	*x*	*y*	*z*	U_{eq}
Ni	0.69010(14)	0.2500	0.40802(16)	0.039
C3	0.8454(8)	0.3137(9)	0.5190(9)	0.051
C33	0.9149(10)	0.3808(11)	0.5843(9)	0.078
N4	0.7827(6)	0.3587(7)	0.4604(7)	0.045
C5	0.7790(10)	0.4812(11)	0.4470(10)	0.067
C6	0.7169(9)	0.5128(11)	0.3571(11)	0.076
C7	0.6093(10)	0.4815(11)	0.3663(10)	0.071
N8	0.5937(7)	0.3569(8)	0.3639(6)	0.050
C9	0.5092(9)	0.3104(10)	0.3363(9)	0.063
C99	0.4217(9)	0.3782(14)	0.3015(11)	0.093
Cl1	0.1257(4)	0.2500	0.4012(5)	0.065
O11	0.1563(13)	0.2500	0.4964(12)	0.100
O12	0.0278(14)	0.2500	0.3896(16)	0.312
O13	0.1652(14)	0.1608(13)	0.3524(11)	0.201
Cl2	0.5980(6)	0.2500	0.6659(5)	0.094
O21	0.6090(14)	0.3376(17)	0.6083(15)	0.243
O22	0.508(3)	0.2500	0.707(2)	0.255
O23	0.674(5)	0.2500	0.712(3)	0.570
OW	0.392(4)	0.2500	0.512(3)	0.402

[a] Numbers in parentheses are errors in the last significant digit(s). $U_{eq} = {}^1/_3\sum_i\sum_j U_{ij}a^*_i a^*_j \mathbf{a}_i\cdot\mathbf{a}_j$.

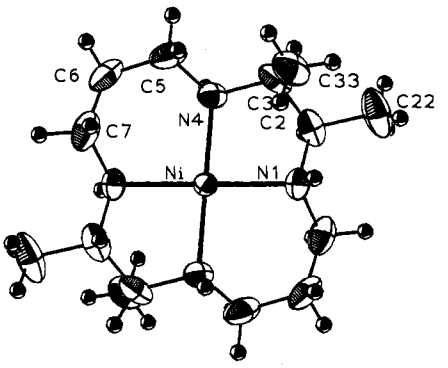

Figure 1. An ORTEP drawing of the cation of *C-RSSR*-[NiHTIM]-(ClO$_4$) (**1**). The thermal ellipsoids are at the 50% probability level. The atom labeling scheme used for ligand in all four structures is presented here. The nickel(I) ion sits on a crystallographic inversion center which relates the labeled atoms to the unlabeled atoms.

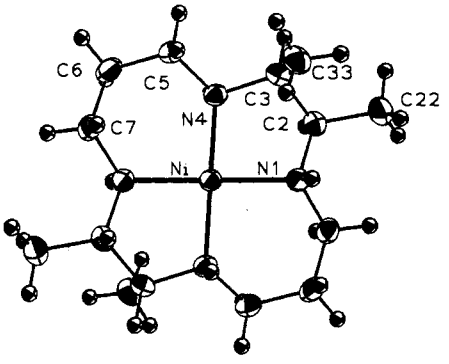

Figure 2. An ORTEP drawing, with the thermal ellipsoids at the 50% probability level, of the cation of *C-RSSR*-[NiHTIM](ClO$_4$)$_2$ (**2**). The nickel(II) sits on a crystallographic inversion center.

to the labeled atoms by an inversion center upon which the nickel cation resides. In both cases the coordination sphere of the nickel is square planar with the four nitrogen atoms of the fourteen membered macrocycle, HTIM, coordinated to the nickel. In each case the ligand shows the *Trans III* configuration, in which the hydrogen atoms on nitrogen atoms of the six membered ring are on the same side of the macrocycle while the hydrogen atoms trans to them are on the opposite sides of the plane. Of the two adjacent methyl groups of the macrocycle one occupies an axial site while the other is equatorial. This

Table 6. Select Bond Lengths and Angles[a] for *C-RSSR*-[NiHTIM](ClO$_4$) (**1**), *C-RSSR*-[NiHTIM](ClO$_4$)$_2$ (**2**), *C-RRSS*-[NiHTIM](ClO$_4$)$_2$ (**3**), and [NiTIM](ClO$_4$)$_2$ (**4**)

	1	2	3	4
Metal Coordination Sphere Distances (Å)				
Ni–N1	2.083(3)	1.969(1)	1.937(3)	
Ni–N4	2.053(3)	1.948(2)	1.944(3)	1.903(8)
Ni–N8				1.882(9)
Ni–O$_{(closet)}$		2.902(3)	3.052(3)	3.128(19)
Metal Coordination Sphere Angles (deg)				
N1–Ni–N4	84.6(1)	85.7(1)	85.7(1)	83.6(4)
N1–Ni–N8				176.2(4)
N4–Ni–N8				96.5(4)
Ligand Distances (Å)				
N1–C2	1.483(5)	1.497(2)	1.486(4)	
C2–C22	1.530(5)	1.528(2)	1.536(4)	
C2–C3	1.532(6)	1.520(2)	1.500(4)	1.487(22)
C3–C33	1.522(5)	1.522(2)	1.516(5)	1.504(15)
C3–N4	1.483(5)	1.494(2)	1.495(3)	1.268(13)
N4–C5	1.466(5)	1.486(2)	1.486(4)	1.444(14)
C5–C6	1.507(7)	1.508(3)	1.500(4)	1.528(17)
C6–C7	1.507(7)	1.510(3)	1.502(5)	1.471(17)
C7–N8	1.477(5)	1.491(2)	1.488(4)	1.469(16)
N8–C9				1.296(13)
C9–C99				1.479(16)
C9–C10				1.410(24)
Ligand Angles (deg)				
C14–N1–Ni	114.2(2)	119.1(1)	117.6(2)	
Ni–N1–C2	105.4(2)	107.5(1)	111.6(2)	
C14–N1–C2	114.2(3)	111.5(1)	110.3(2)	
N1–C2–C22	114.6(3)	114.6(2)	112.2(3)	
C22–C2–C3	111.8(4)	113.6(2)	112.2(3)	
N1–C2–C3	107.3(3)	105.8(1)	108.0(2)	
C2–C3–N4	106.9(3)	104.9(1)	108.1(2)	114(1)
C2–C3–C33	112.5(3)	113.5(2)	112.9(3)	121(1)
C33–C3–N4	110.9(3)	112.4(1)	112.9(3)	124(1)
C3–N4–Ni	107.4(2)	110.0(1)	110.4(2)	112.6(7)
Ni–N4–C5	116.9(2)	121.0(1)	118.9(2)	126.2(8)
C3–N4–C5	115.3(3)	112.2(1)	109.3(2)	121(1)
N4–C5–C6	112.4(3)	111.5(1)	113.1(3)	111(1)
C5–C6–C7	115.1(3)	112.6(1)	112.9(3)	113(1)
C6–C7–N8	111.6(3)	112.2(1)	111.9(2)	112(1)
C7–N8–Ni				123.7(8)
Ni–N8–C9				113.4(8)
C7–N8–C9				123(1)
N8–C9–C10				115(1)
N8–C9–C99				123(1)
C99–C9–C10				122(1)

[a] N8 and C14 are related to N1 and C7 by the symmetry operation $-x, 1-y, -z$, in (**1**); $1-x, 1-y, 1-z$ in (**2**); and $-x, -y, -z$ in (**3**). N1, C2, and C10 are related to N4, C3, and C9 by the symmetry operation $x, {}^1/_2 - y, z$ in (**4**).

C-RSSR-arrangement is found for (**2**) (Ni^{II}) as well as (**1**) (Ni^{I}). The major difference between the two structures due to the different oxidation states of the metal is an increase of about 0.11 Å in the Ni–N bond lengths upon reduction of the metal center. There are two sets of Ni–N bond lengths in these complexes (Table 6). The Ni–N adjacent to the carbon with the equatorial methyl group is 0.02 to 0.03 Å longer than the Ni–N adjacent to the carbon with the axial methyl group. The bond lengths and angles within the macrocycle are similar. Any stress caused in the macrocycle by the increase in Ni–N bond length in (**1**) results in a decrease in the N–C bond lengths. This decrease is about 0.015 Å (3σ), but is observed in all eight C–N bonds in the macrocycles.

Figure 3 is an ORTEP drawing of the cation of *C-RRSS*-[NiHTIM](ClO$_4$)$_2$ (**3**) which is an isomer of (**2**). The difference between these two complexes is that in (**3**) all the methyl groups on the macrocycle are in equatorial positions. Since the environments of all four nitrogens are the same, all the Ni–N bond distances are within one sigma of the average value of 1.940(3) Å.

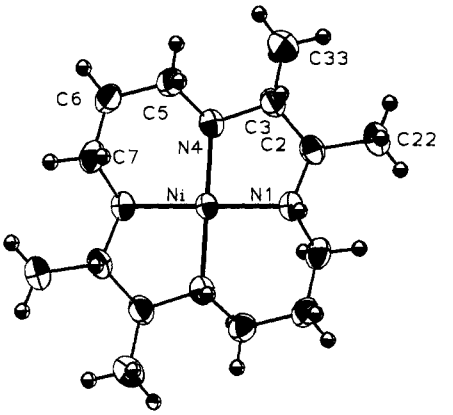

Figure 3. An ORTEP drawing, with the thermal ellipsoids at the 50% probability level, of the cation of *C-RRSS*-[NiHTIM](ClO$_4$)$_2$ (**3**). The nickel(II) sits on a crystallographic inversion center.

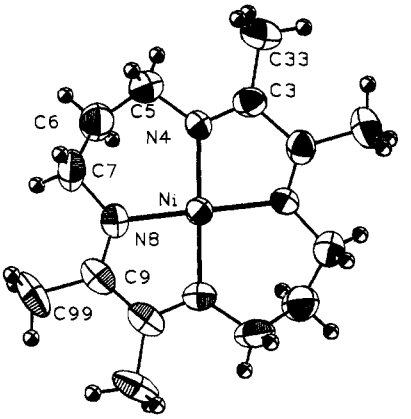

Figure 4. An ORTEP view, with the thermal ellipsoids at the 50% probability level, of the cation of [NiTIM](ClO$_4$)$_2$ (**4**). A crystallographic mirror plane relates the labeled atoms to the unlabeled atoms.

The cation of the parent compound of these complexes, [NiTIM](ClO$_4$)$_2$ (**4**), is presented in Figure 4. The molecule is divided by a crystallographic mirror plane which relates the labeled and unlabeled atoms. The structure is similar to (**3**) but the presence of four N=C imine bonds in the macrocycle results in a decrease in the Ni–N$_{imine}$ bond lengths of 0.048 Å to an average value of 1.892 (9) Å. The nickel atom lies 0.06 Å out of the plane of the four nitrogen atoms. (The nickel is in the plane of the four nitrogens, as required by the crystallographic symmetry, in (**1**), (**2**) and (**3**).)

Spectroscopic Properties. The electronic absorption spectra of the Ni^{II} and Ni^{I} complexes of HTIM and DMC in CH_3CN are shown in Figures 5 and 6, respectively, together with the spectra of their CO adducts. Table 7 summarizes the spectroscopic observations for the Ni^{II}, Ni^{I}, and Ni^{I}–CO complexes.

Acetonitrile Adduct Formation. The equilibrium constants for adduct formation of [Nicyclam]$^{2+}$, [NiDMC]$^{2+}$, and *C-RRSS*-[NiHTIM]$^{2+}$ with acetonitrile in nitromethane are summarized in Table 8.

Electrochemistry and CO binding. The Ni$^{II/I}$ potentials (vs SCE) and equilibrium constants for CO binding in CH_3CN are given in Table 9 together with CO vibrational frequencies. The CO binding constants in CH_3CN are similar to previously published results in DMF.[17]

Discussion

Spectroscopy. Ni(II) complexes with saturated macrocyclic ligands shown in Table 7 are high spin (or a mixture of high

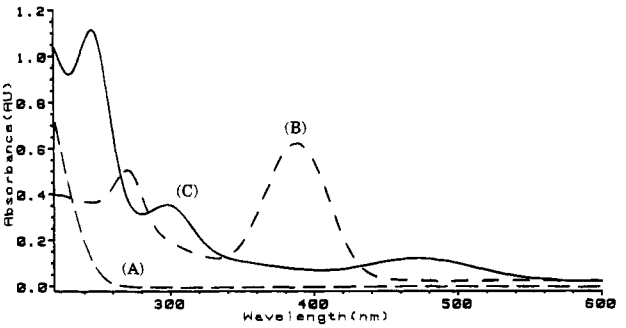

Figure 5. Absorption spectra of *C-RRSS*-$[Ni^{II}HTIM]^{2+}$ (A), *C-RRSS*-$[Ni^{I}HTIM]^{+}$ (B) and *C-RRSS*-$[Ni^{I}HTIM\text{-}CO]^{+}$ (C) in CH_3CN. Ni concentration, 7.14×10^{-4} M; path length, 0.2 cm.

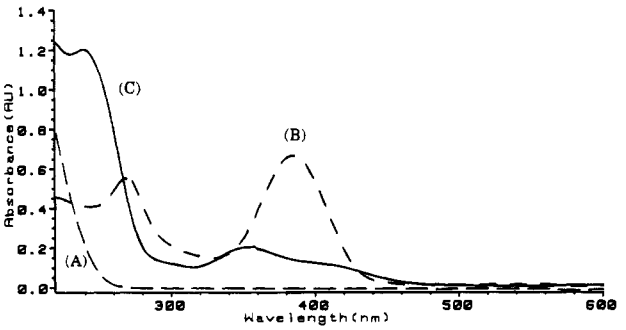

Figure 6. Absorption spectra of $[Ni^{II}DMC]^{2+}$ (A), $[Ni^{I}DMC]^{+}$ (B) and $[Ni^{I}DMC\text{-}CO]^{+}$ (C) in CH_3CN. Ni concentration, 7.97×10^{-4} M; Path length, 0.2 cm.

and low spin) in CH_3CN and low spin in CH_3NO_2, based on the observation by NMR. When square planar, diamagnetic orange crystals of Ni(II) complexes with saturated macrocycles are added to CH_3CN, the crystals become pale green ($[Nicyclam]^{2+}$) or almost white (other complexes) before they dissolve. When dark pink crystals of $[NiTMC](ClO_4)_2$ are dissolved in CH_3CN, the solution turns blue. Numerous spectroscopic and magnetic studies[45-47] have shown that in coordinating solvents the nickel(II) complexes may exist in an equilibrium between the square-planar and the tetragonally distorted octahedral species according to eqs 1-3. The data collected for the equilibrium constant β (Table 8) prove that there is stepwise addition of acetonitrile to $[Nicyclam]^{2+}$, $[NiDMC]^{2+}$ and *C-RRSS*-$[NiHTIM]^{2+}$ in nitromethane solution. It is found that $K_1 < K_2$, which means that the formation of the octahedral bis adduct is preferred over the formation of the five-coordinate mono adduct. The complex cation $[NiDMC]^{2+}$ has the largest β and appears to be the stronger electrophile, as compared to *C-RRSS*-$[NiHTIM]^{2+}$ and especially to $[Nicyclam]^{2+}$. The equilibrium constant β for $[Nicyclam]^{2+}$ of the present study is about a factor of three greater than that reported earlier.[46] One should consider however that the determination of small equilibrium constants by spectrophotometric titration is subject to relatively high error and that the smaller number reported was obtained by magnetic measurements.

$[Nicyclam](ClO_4)_2$, $[NiDMC](ClO_4)_2$ and *C-RRSS*-$[NiHTIM](ClO_4)_2$ have d-d absorption bands in CH_3NO_2 at 454 nm (ϵ = 65 M^{-1} cm^{-1}), 466 nm (ϵ = 61 M^{-1} cm^{-1}), and 460 nm (ϵ = 68 M^{-1} cm^{-1}), respectively. This absorption of $[Nicyclam]^{2+}$ has been assigned to a d-d transition ($^1B_{1g} \rightarrow {}^1B_{2g}$) of the square planar complex.[45] On the other hand, these complexes in CH_3CN have three d-d transitions which have been assigned to a $^3B_{1g} \rightarrow {}^3E_g$ transition around 324 nm for the distorted octahedral complex, a $^1B_{1g} \rightarrow {}^1B_{2g}$ transition for the square-planar complex around 480 nm and a $^3B_{1g} \rightarrow {}^3B_{2g}$ transition around 670 nm for the distorted octahedral complex.[45] A detailed spectrochemical study[51] with series of high-spin $NiLX_2$ (L = macrocyclic ligand, X = Br, Cl, N_3 and NCS) indicates that the high spin species have several absorptions in the visible region. Therefore the

Table 7. Electronic Absorption Spectra of Nickel Complexes in CH_3CN at 25 °C

complex	λ_{max}, nm (ϵ, M^{-1} cm^{-1})	ref
$[Ni^{II}TIM]^{2+}$ (low spin)	415 sh (2240), 396 (2640), 300 sh (820)	20
C-RSRS-$[Ni^{II}TMC]^{2+}$	610 (38), 382 (115), 234 (5900)	this work
$[Ni^{II}diene]^{2+}$ (low spin)	438 (90), 280 (5020), 214 (15800)	20
C-RRSS-$[Ni^{II}HTIM]^{2+}$	670 (4), 480 (10), 324 (14)	this work
C-RRSS-$[Ni^{II}HTIM]^{2+}$ [a]	460 (68)	this work
$[Ni^{II}DMC]^{2+}$	668 (4), 484 (8), 324 (14)	this work
$[Ni^{II}DMC]^{2+}$ [a]	466 (61)	this work
$[Ni^{II}(cyclam)]^{2+}$	660 (4), 456 (26), 370 sh (15), 320 sh (24), 280 sh, 240 sh	this work
$[Ni^{II}(cyclam)]^{2+}$ [a]	454 (65)	this work
C-RSRS-$[Ni^{I}TMC]^{+}$	684 (130), 348 (3370), 250 (3890)	this work
$[Ni^{I}diene]^{+}$	600 sh (1270), 468 (4120), 340 sh (2300), 305 (2930)	20
C-RRSS-$[Ni^{I}HTIM]^{+}$	564 (40), 388 (4340), 270 (3610)	this work
$[Ni^{I}DMC]^{+}$	570 (36), 384 (4010), 268 (3440)	this work
$[Ni^{I}(cyclam)]^{+}$	560 (80), 384 (4400), 267 (4300)	this work
$[Ni^{I}TIM\text{-}CO]^{+}$ [b]	680 sh (3020), 546 (6000), 480 sh (4710), 400 sh (4100), 378 (4420)	20
C-RSRS-$[Ni^{I}TMC\text{-}CO]^{+}$	706 (<100), 450 (680), 350 sh (960)	this work
$[Ni^{I}(diene\text{-}CO)]^{+}$	620 (40), 410 sh (1500), 345 sh (3600), 301 (3300), 238 (8100)	20
C-RRSS-$[Ni^{I}HTIM\text{-}CO]^{+}$	635 sh (27), 470 (790), 296 (2450), 246 (7710)	this work
$[Ni^{I}DMC\text{-}CO]^{+}$	632 (59), 410 sh (960), 352 (1430), 240 (7580)	this work
$[Ni^{I}(cyclam\text{-}CO)]^{+}$	620 (100), 400 sh (940), 348 (1540)	this work

[a] In CH_3NO_2. [b] In C_3H_7CN at −120 °C.

Table 8. Equilibrium Constants for Adduct Formation with Acetonitrile in Nitromethane at 298 K

complex	$\beta = K_1K_2$, M^{-2}	K_1, M^{-1}	K_2, M^{-1}	ref
$[Ni(cyclam)]^{2+}$	0.079 ± 0.004	0.118 ± 0.005	0.669 ± 0.039	this work
$[NiDMC]^{2+}$	0.70 ± 0.04	0.36 ± 0.01	1.9 ± 0.1	this work
C-RRSS-$[NiHTIM]^{2+}$	0.123 ± 0.004	0.059 ± 0.007	2.1 ± 0.2	this work
$[Ni(cyclam)]^{2+}$	0.0241[a]			45
	0.1642[a,b]			45
N-RSRS-$[NiTMC]^{2+}$		1.2[a]		46
		1.2-1.8[a,b]		46, 48-50

[a] The data for β, K_1, and K_2 of the present study are based on spectrophotometric titration according to eqs 1-4. Some of the data taken from literature were determined in pure acetonitrile or DMF. To allow a meaningful comparison, they were divided by [solvent] (K_1) and [solvent]^2 (β), respectively. [b] DMF instead of acetonitrile.

(45) Vigee, G.; Watkins, C. L.; Bowen, H. F. *Inorg. Chim. Acta* **1979**, *35*, 255-259.
(46) Iwamoto, E.; Yoneyama, T.; Yamasaki, S.; Yabe, T.; Kumamaru, T.; Yamamoto, Y. *J. Chem. Soc., Dalton Trans.* **1988**, 1935-1941.
(47) Busch, D. H. *Acc. Chem. Res.* **1978**, *11*, 392.
(48) Röper, J.; Elias, H. *Inorg. Chem.* **1992**, *31*, 1210-1214.
(49) Lincoln, S. F.; Hambley, T. W.; Pisanillo, D. L.; Coates, J. H. *Aust. J. Chem.* **1984**, *37*, 713.
(50) Crick, I. S.; Tregloan, P. A. *Inorg. Chim. Acta* **1988**, *142*, 291.
(51) Martin, L. Y.; Sperati, C. R.; Busch, D. H. *J. Am. Chem. Soc.* **1977**, *99*, 2968-2981.

Table 9. Carbon Monoxide Binding Constants[a] and Carbonyl Vibrational Frequencies in CH_3CN at 25 °C

compd	$E_{1/2}$, V vs SCE	K_{CO}, M^{-1}	ν_{CO}, cm^{-1}	ref
$[NiTIM]^+$	−0.498	$(1.3 \pm 0.3) \times 10^2$	2012	20
C-RSRS-$[NiTMC]^+$	−0.837	$(1.2 \pm 0.4) \times 10^5$	1967	this work
$[Ni(diene)]^+$	−1.215	$(5.6 \pm 1.5) \times 10^4$	1962	20
C-RRSS-$[NiHTIM]^+$	−1.430	$(9.0 \pm 2.0) \times 10^4$	1939	this work
$[NiDMC]^+$	−1.445	$(1.8 \pm 0.4) \times 10^5$	1956	this work
$[Ni(cyclam)]^+$	−1.445	$(2.8 \pm 0.6) \times 10^5$	1955	20

[a] For *C-RSRS*-$[NiTIM]^+$, K_{CO} is defined by the following reaction: $Ni^{II}(TIM^{\bullet})^+ + CO \rightleftharpoons Ni^{I}TIM\text{-}CO^+$. The first reduction is the ligand reduction in the complex.

absorption at 480 nm could be assigned to the $^3B_{1g} \rightarrow {}^3E_g$ transition of the distorted octahedral complex instead of the $^3B_{1g} \rightarrow {}^3B_{2g}$ transition of the square-planar complex which is in equilibrium with the octahedral adduct. In fact the absorption maximum shifts by ~20 nm when the solvent is changed from CH_3NO_2 to CH_3CN for $[NiDMC](ClO_4)_2$ and *C-RRSS*-$[NiHTIM](ClO_4)_2$. The molar absorptivities of $[NiDMC](ClO_4)_2$ and *C-RRSS*-$[NiHTIM](ClO_4)_2$ in CH_3CN are smaller than that of $[Nicyclam](ClO_4)_2$. Since β for $[Nicyclam]^{2+}$ is smaller than β for $[NiDMC]^{2+}$ and $[NiHTIM]^{2+}$ (0.079 compared to 0.70 and 0.123 M^{-2}, respectively), a larger contribution from the square-planar species is possible. But more than 90% of $[Nicyclam]^{2+}$ is six-coordinate in CH_3CN. Since the presence of cis-$[Nicyclam]^{2+}$ and the five-coordinate species should be ruled out, a possible explanation for the high absorptivity of $[Nicyclam]^{2+}$ in CH_3CN could be the presence of a certain fraction of the *Trans I* isomer. In equilibrated aqueous solution this isomer constitutes about 15% of the total complex and is not in rapid equilibrium with a high-spin form.[52]

The UV-vis spectra of the CH_3CN solutions of $[Ni^{I}cyclam]^+$, $[Ni^{I}DMC]^+$, and *C-RRSS*-$[Ni^{I}HTIM]^+$ are quite similar to each other. The d-d transitions of these complexes occur at 560–570 nm, which means that they are by about 100 nm red-shifted compared to the square-planar Ni(II) complexes. This indicates that the ligand-field strength decreases upon reduction of the metal. The molar absorptivities of the d–d transition bands at 570 nm for these Ni(I) complexes are almost the same as those for the square-planar Ni(II) complexes. As can be seen from Figure 1, the x-ray structure of *C-RSSR*-$[Ni^{I}HTIM]^+$ (**1**) is square-planar and, therefore, these Ni(I) complexes likely have square-planar geometry in solution with longer Ni–N bond distances (Ni–N distances in the crystal are 2.083(3) and 2.053(3) Å) than the Ni(II) complexes. Intense bands at ~384 nm and ~270 nm of these Ni(I) complexes can be classified as charge-transfer bands.

As can be seen from Figures 5 and 6, and Table 7, the $[NiHTIM\text{-}CO]^+$ spectrum is quite different from that of $[Nicyclam\text{-}CO]^+$ and $[NiDMC\text{-}CO]^+$. $[NiHTIM\text{-}CO]^+$ has an absorption at 470 nm and no absorptions at ~400 and ~350 nm. $[Nicyclam\text{-}CO]^+$ and $[NiDMC\text{-}CO]^+$ have absorptions at ~400 and ~350 nm, but not at 470 nm. When CO was introduced into the solutions of $[Nicyclam]^+$ and $[NiDMC]^+$, prepared by Na–Hg in CH_3CN under vacuum, the color of the solutions changed from olive to brownish orange. Within 30 s, the color then changed to green. The second step of the color change to green did not occur in the solution of $[NiHTIM\text{-}CO]^+$. The similar change of the spectrum for $[Nicyclam\text{-}CO]^+$ has been detected in the reaction of CO with $[Nicyclam]^+$ produced by pulse radiolysis and flash photolysis in H_2O.[53] The change might be due to a conformational change to a more stable species.

Electrochemistry. Equilibrium constants for CO binding to various nickel macrocycles ([Ni] = 1 mM) in CH_3CN, determined by the electrochemical method, are given in Table 9 together with CO vibrational frequencies. Gagné et al. reported[17] CO binding constants of several Ni(I) macrocyclic complexes in DMF and carbonyl vibrational frequencies in pyridine: $[NiTIM]^+$, $K_{CO} = 1.7 \times 10^2\ M^{-1}$, $\nu_{CO} = 2020\ cm^{-1}$; $[Nidiene]^+$, $4.7 \times 10^4\ M^{-1}$, $1962\ cm^{-1}$. The CO binding constants and CO vibrational frequencies are very similar for CH_3CN, DMF and pyridine solvents. As can be seen from Table 9, CO stretching frequencies decrease and CO binding constants increase as NiL^+ becomes a more powerful reductant. This trend is consistent with the backbonding interaction in the binding of CO to nickel. There are two exceptions in this trend: K_{CO} of $[NiTMC]^+$ and ν_{CO} of $[NiHTIM]^+$. Recently Balazs and Anson reported K_{CO} of $1.1 \times 10^6\ M^{-1}$ for $[NiTMC]^+$ in H_2O,[54] which is even greater than that of $1.2 \times 10^5\ M^{-1}$ in CH_3CN. The stronger binding than that expected from the reduction potential could be due to the macrocycle conformation that protects the bound CO in the cavity of four methyl groups. Although the solvent effect was small in the case of $[Co^{I}diene]^+$ ($K_{CO} = 1.9 \times 10^8\ M^{-1}$ in CH_3CN,[41] $K_{CO} = 1.6 \times 10^8\ M^{-1}$ in H_2O),[55] the solvent may play an important role in determining the conformation of the TMC macrocycle. The small ν_{CO} for *C-RRSS*-$[NiHTIM\text{-}CO]^+$ is striking. As mentioned above, the UV-vis spectrum of $[NiHTIM\text{-}CO]^+$ is quite different from those of $[Nicyclam\text{-}CO]^+$ and $[NiDMC\text{-}CO]^+$, despite of the fact that all these square-planar Ni(I) complexes have similar absorption spectra. In order to study the structural differences of these CO adducts, a crystallization was attempted, but it was unsuccessful.

Structures. The bond lengths of 2.083(3) and 2.053(3) Å observed in *C-RSSR*-$[NiHTIM](ClO_4)$ (**1**) are similar to the Ni–N_{amine} value of 2.066(6) Å observed in $[Nidiene]^+$. The increase of 0.11 Å observed in the Ni–N_{amine} bond lengths upon reduction of *C-RSSR*-$[NiHTIM](ClO_4)_2$ (**2**) is similar to the increase of 0.13 Å observed for $[Nidiene]^+$ and $[Nidiene]^{2+}$. This is in contrast to the observations of Suh et al.[21] on the $Ni^{I/II}$ system of polyaza macrotricyclic ligands in which no increase in bond length is observed upon reduction of the nickel cation but a separation into shorter and longer Ni^{I}–N bond lengths are observed. (It appears that in at least one of their cases the ligand also is in two different conformations in the two oxidation states, which may account for some of their observed changes in the Ni–N bond lengths.) In the present case, two different Ni–N bond lengths (differing by 0.030 Å in the nickel(I) complex and 0.021 Å in the nickel(II) complex) are observed. This can be attributed to the presence of an equatorial and axial methyl group, respectively, on the carbon adjacent to the coordinated nitrogen atom. In *C-RRSS*-$[NiHTIM](ClO_4)_2$ (**3**) where all the methyl groups are in equatorial positions only one Ni(II)–N bond length is observed. Thus it can be seen that the conformation of the macrocycle has an effect on the Ni–N bond lengths. This was observed previously in the structures of *racemic* and *meso*-$[Nidiene]^{2+}$ in which the change in the conformation of the macrocycle resulted in a change of 0.023 Å in the Ni–N_{amine} bond length.[26] As has been shown previously, the fourteen membered macrocycles of this type have the ability to adjust to a large number of metal to ligand bond lengths and also have the ability to bend so that they can also coordinate in a *cis* arrangement. The last structure reported here, $[NiTIM](ClO_4)_2$ (**4**), is a tetraene complex in

(52) Connolly, P. J.; Billo, E. J. *Inorg. Chem.* **1987**, 26, 3224.
(53) Kelly, C. A.; Mulazzani, Q. G.; Venturi, M.; Blinn, E. L.; Rodgers, M. A. To be submitted for publication.
(54) Balazs, C. B.; Anson, F. C. *J. Electroanal. Chem.* **1993**, *361*, 149–157.
(55) Creutz, C.; Schwarz, H. A.; Wishart, J. F.; Fujita, E.; Sutin, N. *J. Am. Chem. Soc.* **1991**, *113*, 3361–3371.

which four methyl groups occupy equatorial sites. Only one Ni−N bond length is observed and it is 0.048 Å shorter than that observed in the saturated macrocycle complex.

The occurrence of two sets of Ni−N bond distances are quite common in the square-planar nickel complexes studied previously and in this work. However the structural changes associated with the reduction of Ni(II) to Ni(I) in square-planar complexes can be classified in three ways: (1) expansion of Ni−N distances; (2) distortion of nickel core; (3) both expansion and distortion. The complex with flexible symmetric ligand such as HTIM shows only expansion of the core. Distortion seemed to occur for complexes with unsaturated ligands and rigid ligands. The origin of the distortion in F430, F430M and Ni(I) isobacteriochlorin could be an adjustment between the steric requirements of the ligand and the expansion of the nickel core associated with a decrease of the ligand-field strength.

Acknowledgment. We thank Drs. Bruce Brunschwig and Carol Creutz for their comments. We also acknowledge Drs. C. A. Kelly, Q. G. Mulazzani, M. Venturi, E. L. Blinn, and M. A. Rodgers for making ref 53 available prior to publication. This research was carried out at Brookhaven National Laboratory under contract DE-AC02-76CH00016 with the U.S. Department of Energy and supported by its Division of Chemical Sciences, Office of Basic Energy Sciences. The work carried out at the Technische Hochschule Darmstadt was supported by the Deutsche Forschungsgemeinschaft, Verband der Chemischen Industrie e. V., and Otto-Röhm-Stiftung.

Supplementary Material Available: Tables of crystallographic data collection parameters, anisotropic thermal parameters for non-hydrogen atoms, calculated hydrogen atom positions, and bond distances and angles and Figure S1 (overlay of **1** and **2**) (12 pages). Ordering information is given on any current masthead page.